Generation of deuteron beams from laser-driven thin foils for neutron radiography

Chengkun Huang

Advanced Accelerator Concepts 2026
UCLA
07/27/26

Acknowledgements: M. Alvarado Alvarez, S. H. Batha, D. P. Broughton, A. Junghans, R. Reinovsky, T. R. Schmidt, Z. Wang, C.-S. Wong, B. Wolfe, B. Wyatt; LANL and University of Michigan target fabrication teams; Y. Hayashi, H. Kim, V. Lelasseux and J. Strehlow

Laser-driven neutron sources provide flexible, short-pulse, high flux neutrons in a compact setup

- Many applications (radiography, assay and active interrogation of SNMs, nuclear photonics, etc.) require neutron sources that are compact with high yield and angular flux
- Traditional reactor-based or spallation neutron sources are huge and expensive. Radioactive sources are small but limited in yield/flux

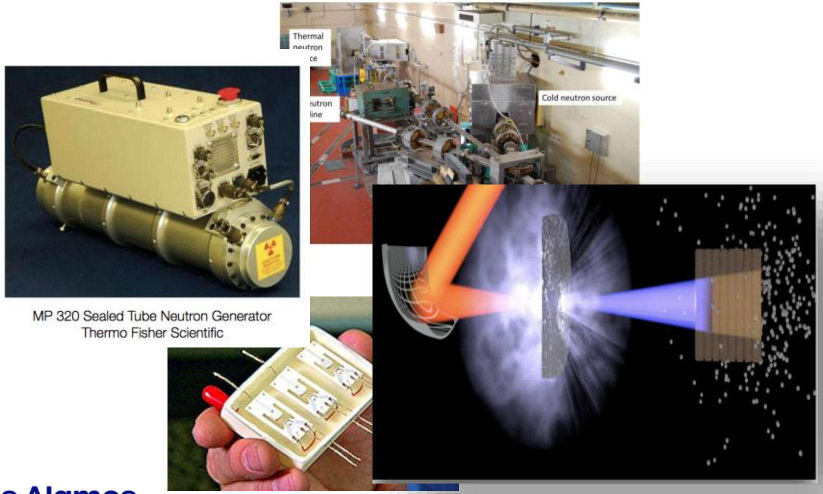

MP 320 Sealed Tube Neutron Generator
Thermo Fisher Scientific

Survey of pulsed power and laser-driven neutron sources

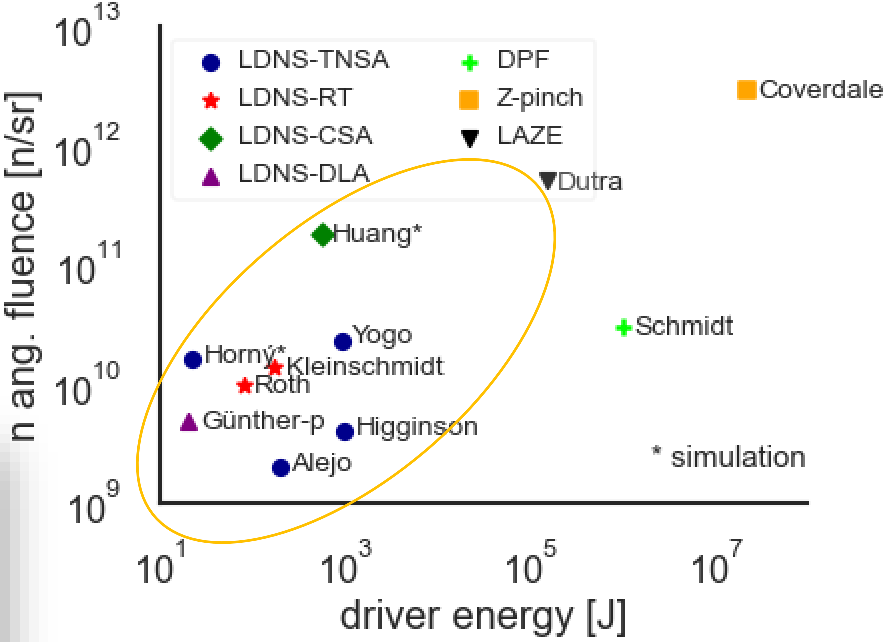

Multi-species radiography with laser driver

- **Peta-watt laser accelerated particles offer promise of a single technology to produces electrons, x-rays, protons and neutrons from very compact sources**
- **A series of experiments are being conducted at OMEGA-EP to characterize laser-driven sources and radiography performance**:

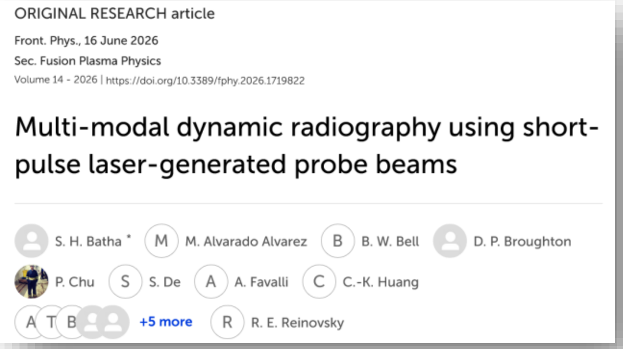
ORIGINAL RESEARCH article

Front. Phys., 16 June 2026
Sec. Fusion Plasma Physics
Volume 14 - 2026 | https://doi.org/10.3389/fphy.2026.1719822

Multi-modal dynamic radiography using short-pulse laser-generated probe beams

S. H. Batha * M. Alvarado Alvarez B. W. Bell D. P. Broughton P. Chu S. De A. Favalli C.-K. Huang +5 more R. E. Reinovsky

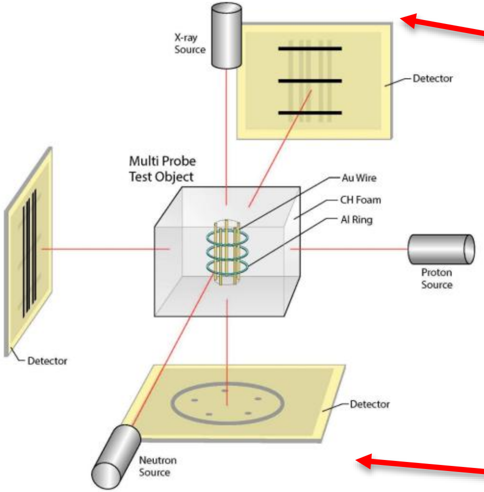

- X-ray sources characterization and elementary dynamic radiography of a shock experiment (*Broughton et al., AIP Advances 15, 055023, 2025*)
- Proton source characterization and elementary dynamic radiography (*Huang et al., Phys. Plasmas 32, 033107, 2025*)
- Combined x-ray and proton sources to explore cross-talk and background issues, and test multiple-species dynamic radiography (*Wong, HED Phys. 52, 101133, 2024*)
- Experiments on laser driven neutron sources is being developed (*Huang et al., APL. 120, 024102, 2022*)

Ion Beam Production Targets for Pitcher-Catcher

Pitcher Catcher

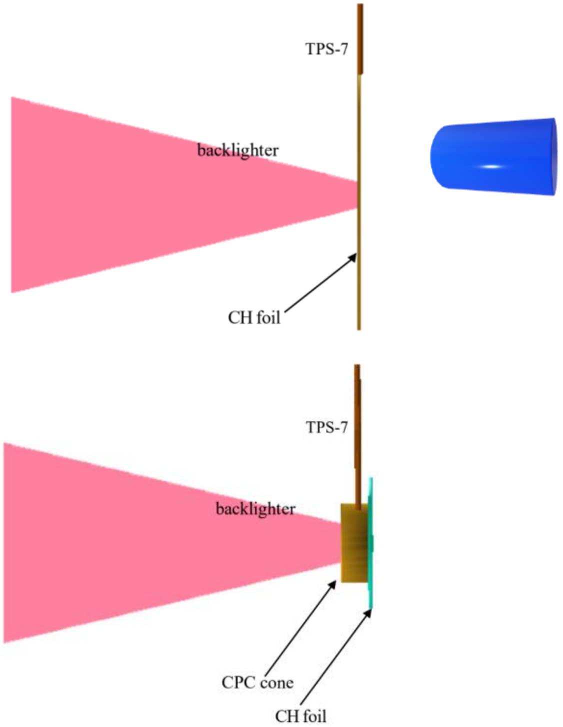

CD foam/film

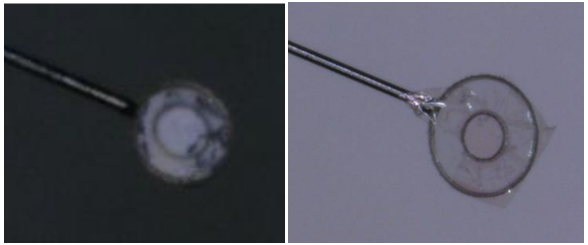

CPC cone*

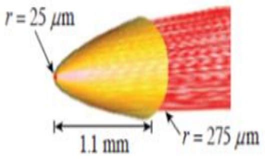

* MacPhee et al., Optica (2020).

Target	Thickness (nm)	Note
CH	2000	film
	500/600/750	W/O CPC
	600	CPC (25/16um tip)
CD	500/700/800	film
	25000	Foam (w/ Al)

CD film production and characterization

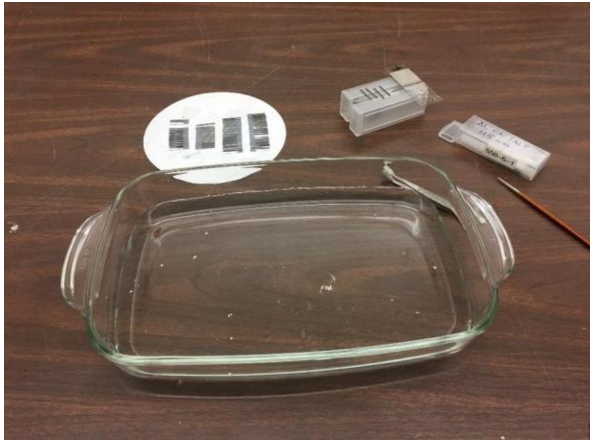

DI water with floating d-PS on Al film squares. In the back, empty targets are shown on the left and drying targets on the right.

Profile measurement via neutron reflectivity

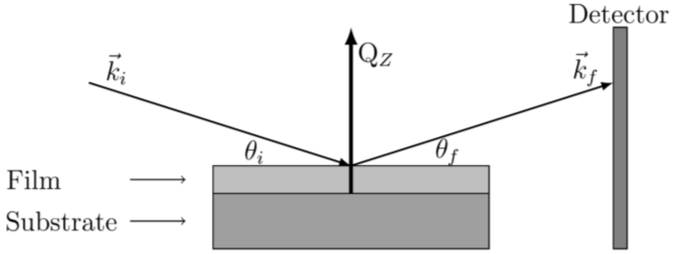

Figure 3.1: Incoming and outgoing wave vectors

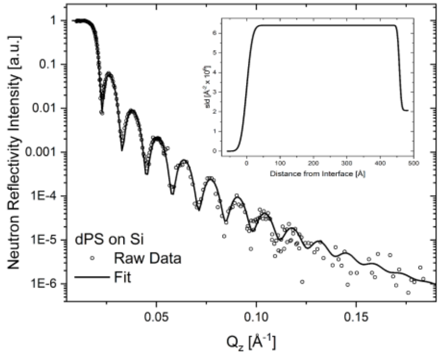

(left) Reflectivity (R vs. Q_z) profile for spin coated film of ~10 mg of d-PS in 1 g of toluene (2000 rpm), (right, top) fitted reflectivity curve and (right, bottom) corresponding SLD profile.

Omega EP experimental setup

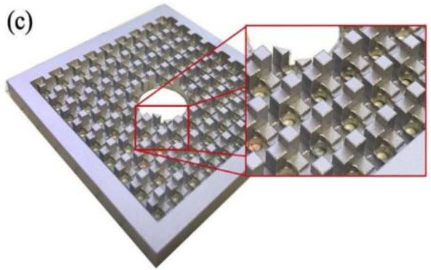

PROton Beam Imager and Energy Spectrometer (PROBIES)

Primary diagnostics:

- Spectrum : Thomson parabola
- Dose profile (energy dependent): PROBIES

Short pulse parameters: 75-500 J, 0.7 ps

Radiochromic film

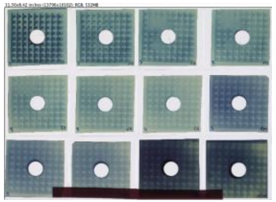

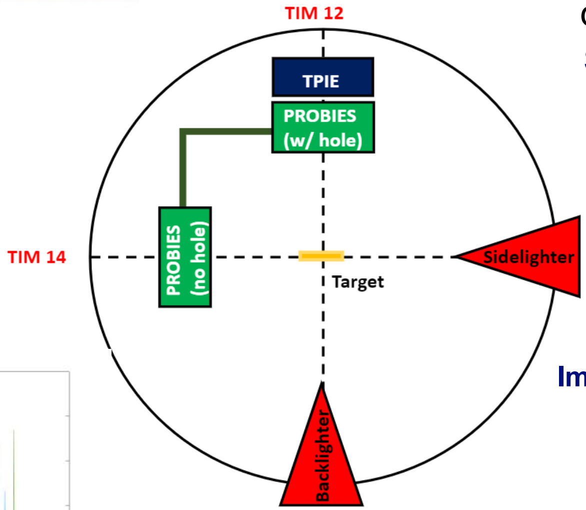

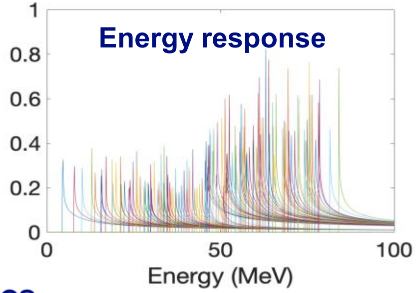

Image Plate

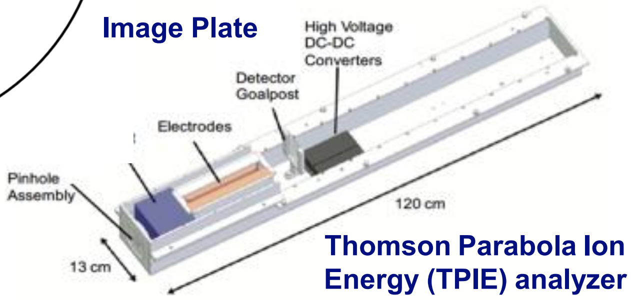

Thomson Parabola Ion Energy (TPIE) analyzer

TR IP calibration data for proton/deuteron

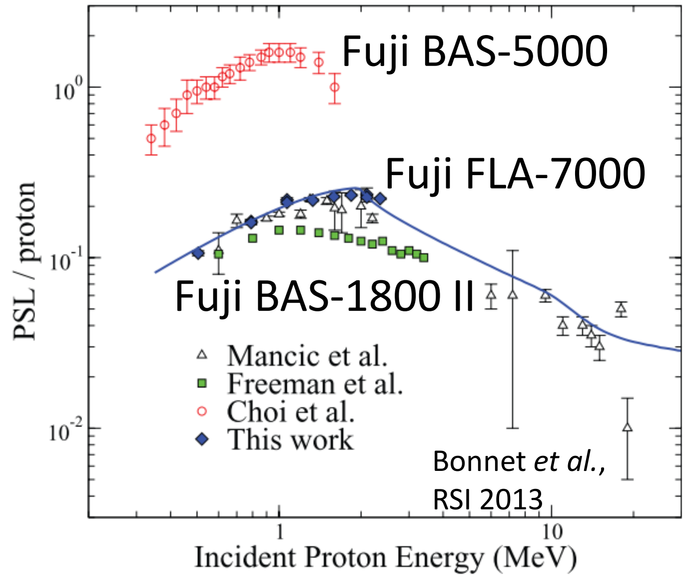

FIG. 5. Response functions of TR IPs. Our work is compared to previous works.

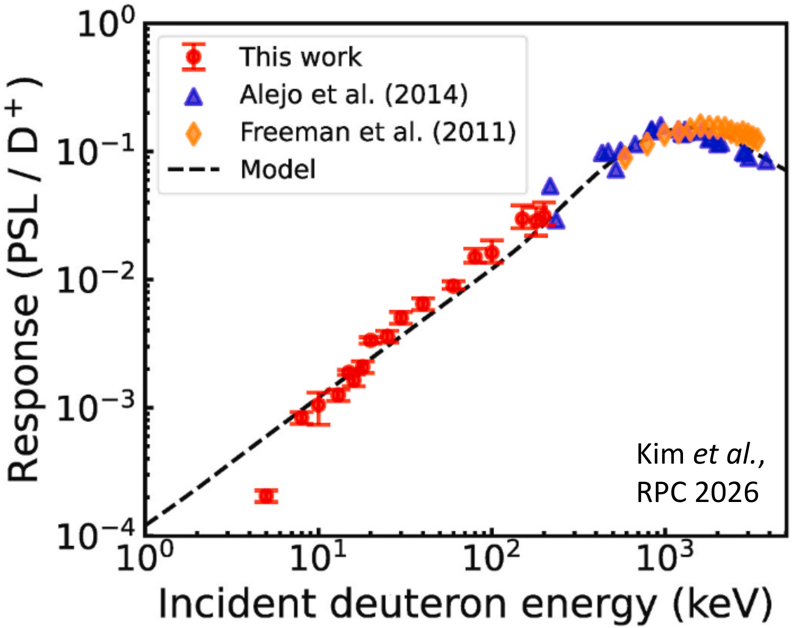

There is a lack of reliable TR IP calibration data for deuteron, especially for the energy range and scanner in our Omega EP experiments.

Scanner sensitivity calibration

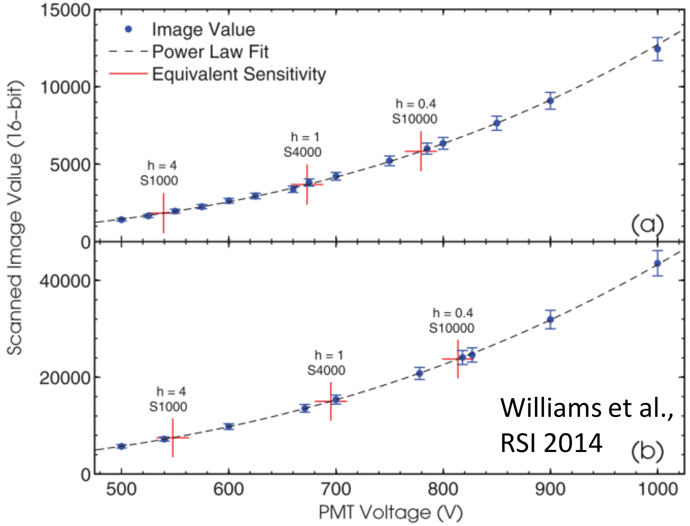

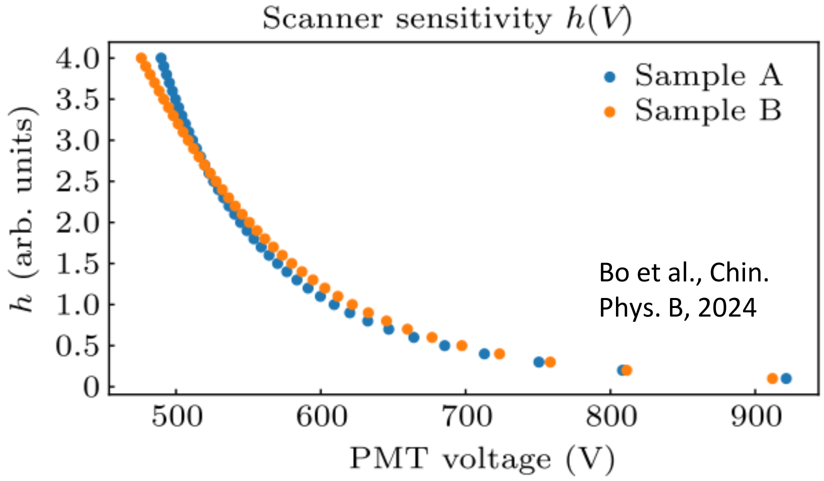

Fig. 4. Sensitivity curve of GE Typhoon FLA 7000 scanner.

- Often differences in IP sensitivity calibration is attributed to the scanner used.
- Scanner calibration usually is not known or reported in literature

$$\mathrm{PSL} = \left(\frac{G}{2^{16}-1}\right)^2 \left(\frac{R_{\mu m}}{100}\right)^2 h(V)\, 10^{L/2}$$

PSL fading for TR IP

- IP fading has been measured in a variety of conditions and setup.
  - General qualitative agreement (fast initial fading & slower fading over long time scale)
  - Some experiments indicate that the fading is quasi-independent of the nature of the radiation source and its energy
  - Still it can vary substantially
- Bonnet’s measurement appears to be most relevant to our experiment

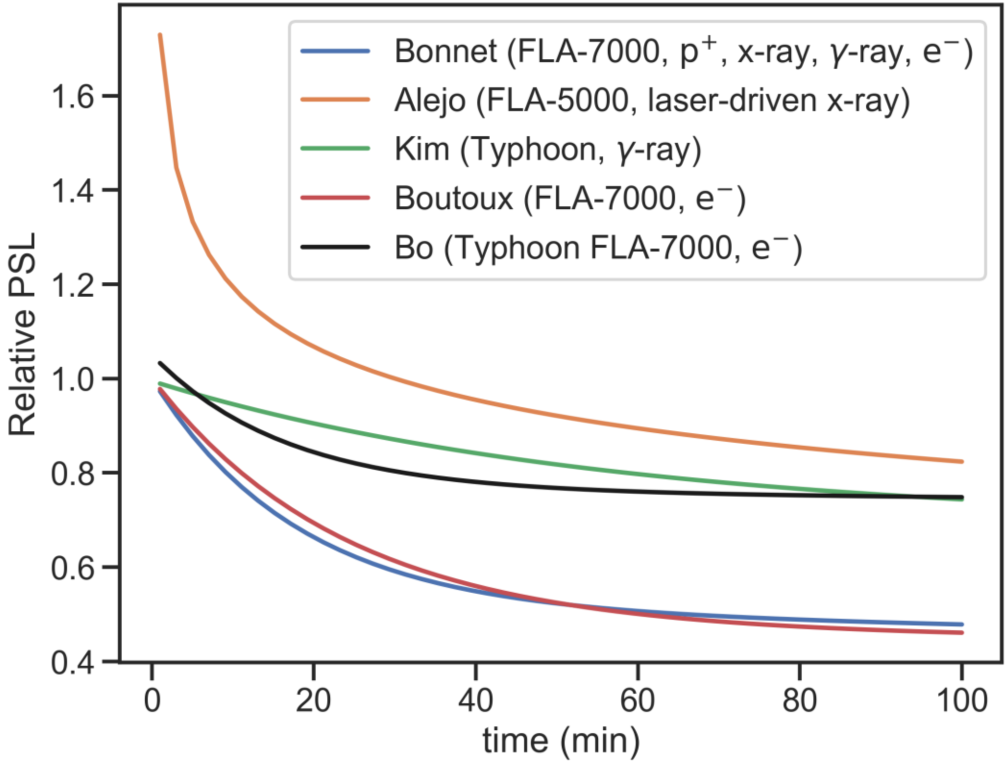

IP sensitivity models for deuteron

- Alejo's empirical fit
  - Up to 8 MeV

$$\mathrm{PSL}_{30}/\mathrm{D}^{+} = \begin{cases} 0.0877\,E_d & E_d < 1.862\ \mathrm{MeV} \\ 0.2115\,E_d^{-0.4363} & E_d \geq 1.862\ \mathrm{MeV} \end{cases}$$

- Bonnet's model

$$R(E_d) = \alpha \int_0^W \frac{dE_{dep}(z, E_d)}{dz} \exp(-z/L)\,dz$$

TR IP, W = 50µm

From SRIM/MCNP/GEANT4: $dE_{dep}(z, E_d)/dz$

Kim et al, 2026: (α, L) = ((1.39 ± 0.07) ×10^{-4} PSL/keV, (14.2 ± 3.7)µm)
(caveats: Alejo data not correctly plotted, no fading correction)

- Birks model
  - Good for light ions
  - no fading correction

$$R(E_d) = \alpha \int_0^W \frac{dE_{dep}/dz}{1 + B|dE_{dep}/dz|} \exp(-z/L)\,dz.$$

α = 2.4 × 10−4 PSL/keV

B = 0.15Å/eV   L = 44µm

Energy deposition by secondary electron (EDSE) model

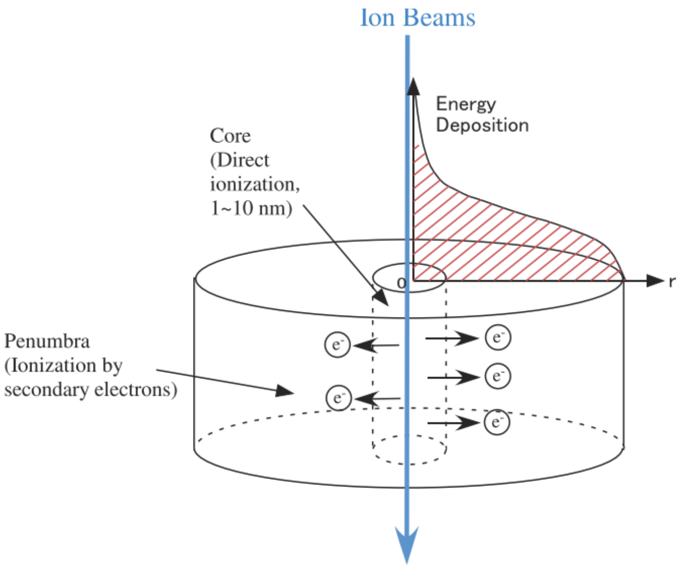

Y. Hayashi et al., “Evaluation of imaging plate sensitivities to ion beams,” *Rev. Sci. Instrum.*, vol. 96, no. 9, p. 093306, Sep. 2025.

$$\frac{dT_e}{dx} = \pi {r_q}^2 \Phi_q + I_P,$$

$$I_P \equiv \int_{r_q}^{\Gamma_{max}} \Psi_P(r) \times 2\pi r dr.$$

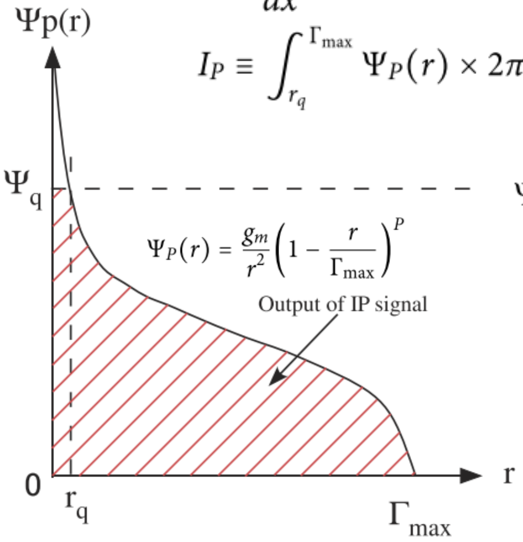

$$\Psi_P(r_q) = \frac{g_m}{{r_q}^2}\left(1 - \frac{r_q}{\Gamma_{max}}\right)^P \equiv \Phi_q.$$

$$\Gamma_{max} = \frac{5.025 \times 10^{-12} A}{0.182 \rho Z^{8/9}} \times \left(\frac{4 m_e E_{ion}}{M}\right)^{5/3}$$

$$R(E_d) = \alpha \int_0^W \frac{dT_e}{dz}\left(1 - f_1 \frac{dT_e/dz}{f_2 + dT_e/dz}\right) \exp(-z/L) dz$$

The solution of EDSE model is applicable to difference ion species, for which $(\alpha, \Phi_p, f_1, f_2)$ can be calibrated.

IP calibration using EDSE model

TABLE III. Parameters for IP scanners.

	TR			SR	
	BAS-1800	FLA-7000	FLA-5000	BAS-1800	FLA-7000
K	2.28×10^{-3}	2.51×10^{-3}	2.06×10^{-3}	5.60×10^{-3}	4.20×10^{-3}
f_1	0.915	0.937	0.971	0.903	0.925
f_2	3.23×10^{-4}	2.70×10^{-4}	8.13×10^{-4}	3.72×10^{-5}	3.32×10^{-4}
Φ_q	4.72×10^{12}	4.43×10^{12}	1.17×10^{9}	6.93×10^{7}	2.47×10^{8}

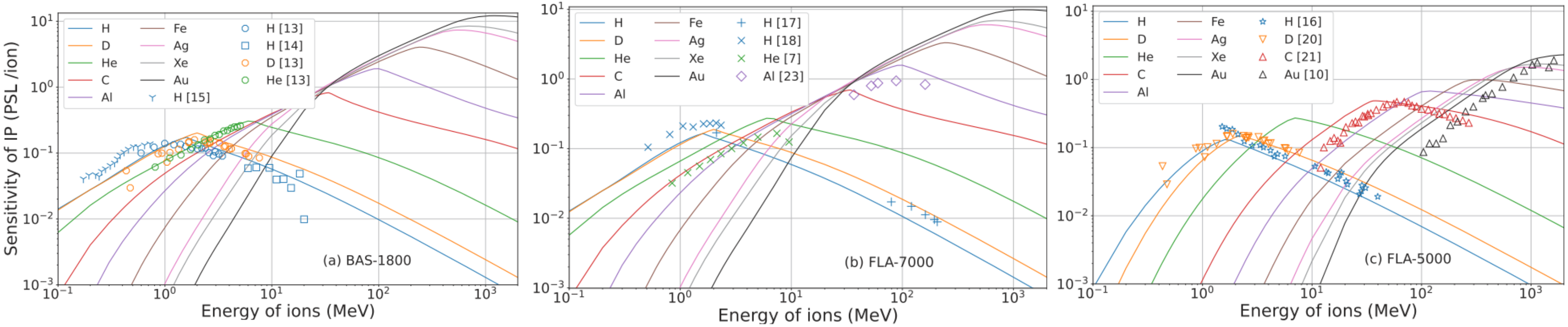

Fading correction not applied.

EDSE model compared to p+/D+ calibration data with IP fading correction

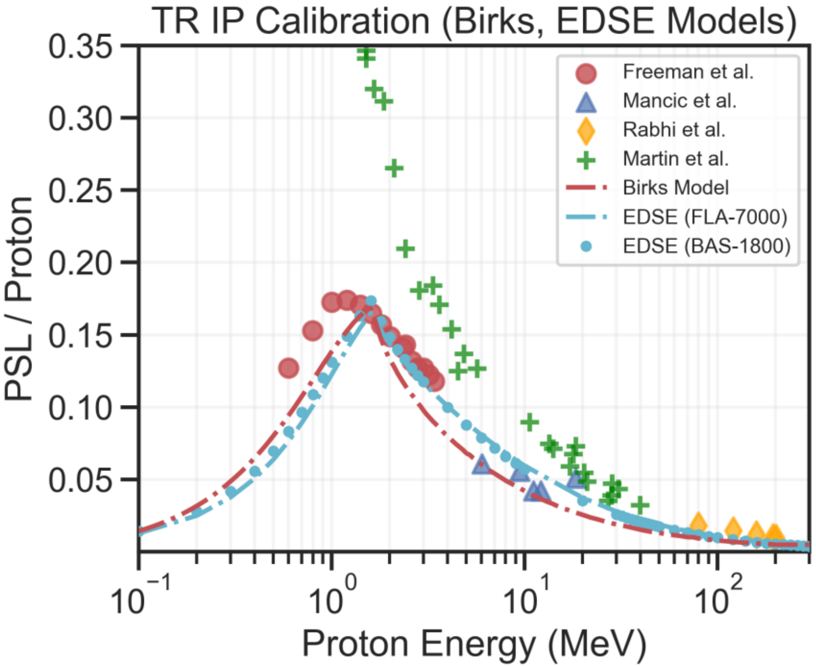

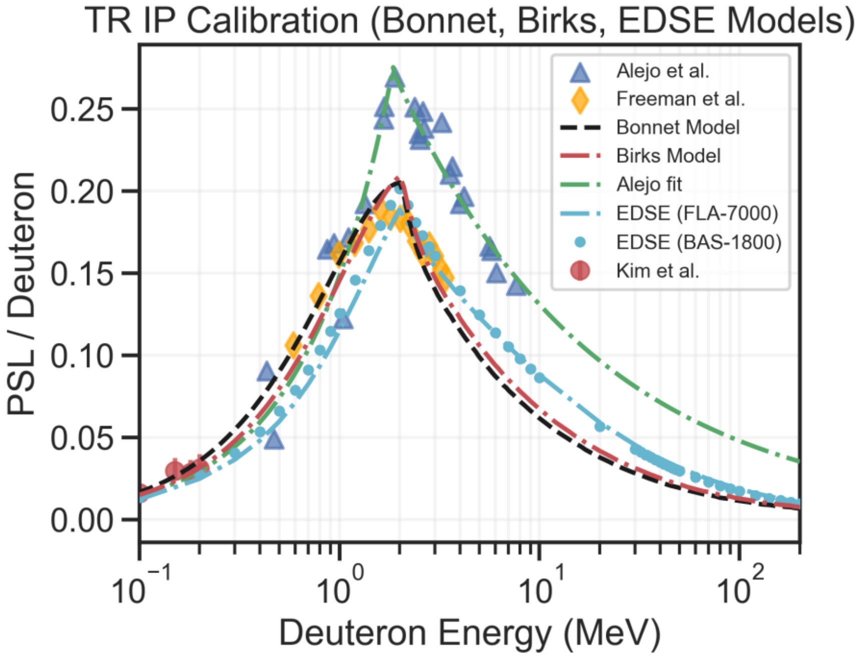

Bonnet's measurement is used for IP fading correction.

Los Alamos NATIONAL LABORATORY

Proton/deuteron spectrum from CD film targets

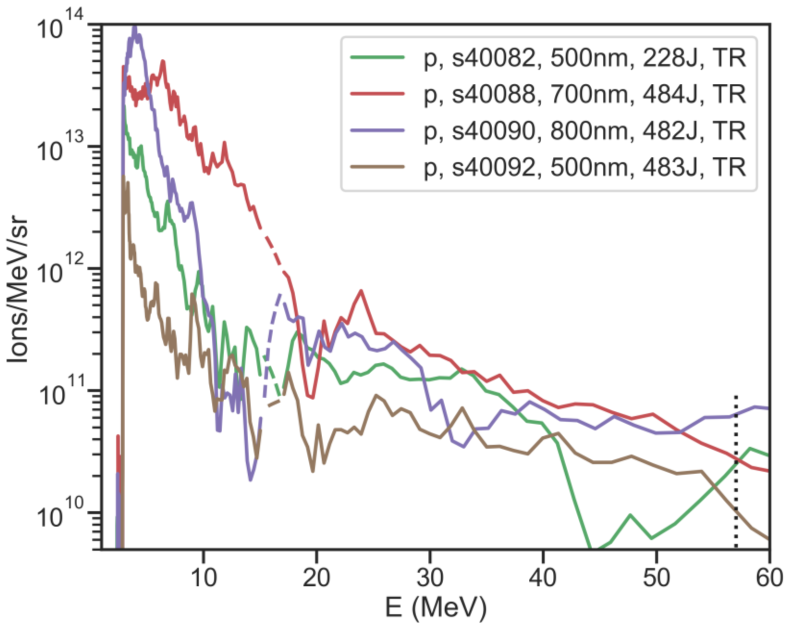

p/sr = 2.18e+14, # part = 2.09e+13,
avg. ion energy= 7.53 MeV,
total beam energy = 25.1 J

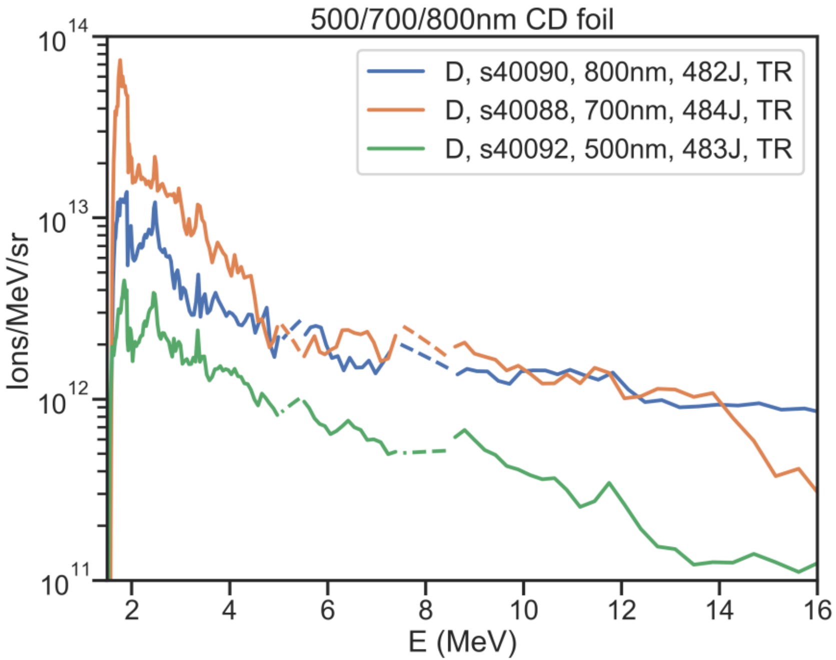

d/sr = 5.95e+13, # part = 5.68e+12,
avg. ion energy= 4.30 MeV,
total beam energy = 3.91 J

Be/LiF converter optimization with proton+deuteron beam

Goals: Maximize neutrons in 10-degree half-angle cone on surface of 10cm radius sphere, minimize converter radius

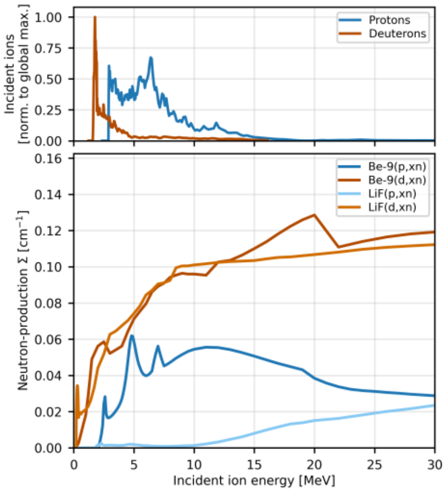

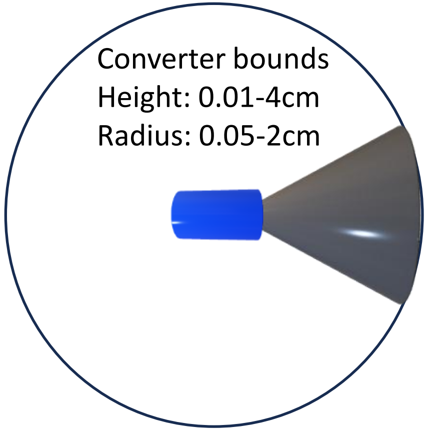

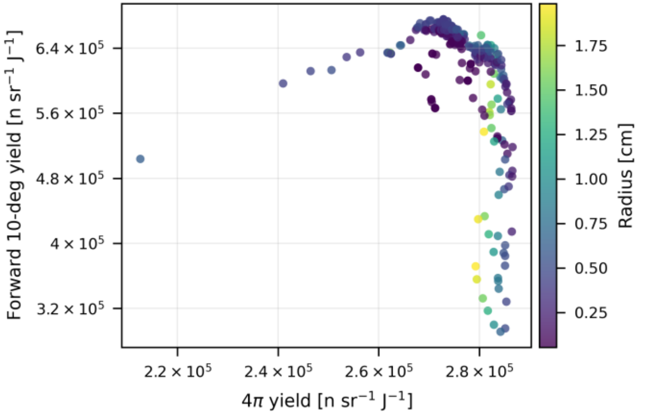

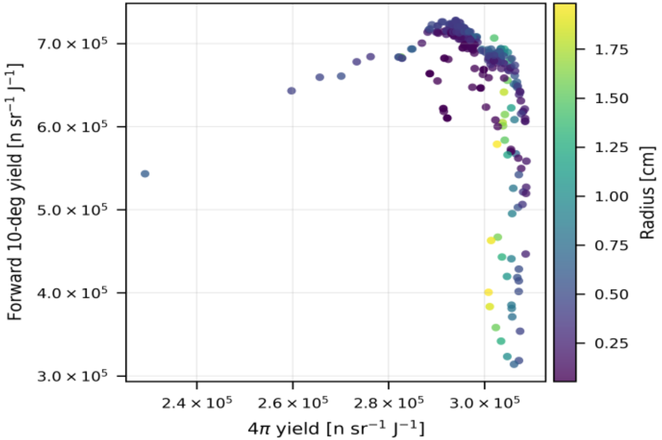

Genetic optimizer parameters:
crossover probability = 0.75
mutation probability = 0.25
per-gene mutation probability = 0.2
Gaussian mutation sigma = 1
8 generations with 40 geometries per generation

Conclusion

- Up to ~16 MeV (filter cut-off) deuteron is detected from sub-micron CD films
- An optimal yield of 5.95×10^{13}/sr and 5.68×10^{12} deuterons/shot are measured from the 700 nm CD film among target thickness in the range of 500-800 nm.
- A large number of protons also present in the ion beam; total energy efficiency of the ion beam is $\sim$ 6%
- IP calibration for proton/deuteron based on a physic (EDSE) model
- The optimized converters can produce significantly enhanced forward neutron yield, reaching 2.85×10^9 n sr^{-1} $shot^{-1}$ in the forward 10° cone for a Be-9 converter and 3.27×10^8 n sr^{-1} $shot^{-1}$ for a LiF converter.